Land Use Influences Carbon Fluxes in Northern Kazakhstan

Jorge F. Perez-Quezada,[1] Nicanor Z. Saliendra,[2] Kanat Akshalov,[3] Douglas A. Johnson,[4] and Emilio A. Laca[5]

Authors are [1]Assistant Professor, Departamento de Ciencias Ambientales y Recursos Naturales Renovables, Universidad de Chile, Santiago, Chile; [2]Research Plant Physiologist, US Department of Agriculture Forest Service Northern Research Station, Institute for Applied Ecosystem Studies, Rhinelander, WI 54501, USA; [3]Senior Researcher, Baraev Kazakh Research Institute for Grain Farming, Shortandy, Kazakhstan; [4]Plant Physiologist, USDA–Agricultural Research Service, Forage and Range Research Lab, Utah State University, Logan, UT 84322, USA; and [5]Professor, Department of Plant Sciences, University of California Davis, Davis, CA 95616, USA.

Abstract

A mobile, closed-chamber system (CC) was used to measure carbon and water fluxes on four land-use types common in the Kazakh steppe ecoregion. Land uses represented crop (wheat or barley, WB), abandoned land (AL), crested wheatgrass (CW), and virgin land (VL). Measurements were conducted during the growing season of 2002 in northern Kazakhstan at three locations (blocks) 15–20 km apart. The CC allowed the measurement of the carbon flux components of net ecosystem exchange (NEE), ecosystem respiration (R_E) and soil respiration (R_S), together with evapotranspiration (ET). Nonlinear regression analyses were used to model gross primary production (GPP) and ET as a function of photosynthetically active radiation (Q); R_E and R_S were modeled based on air (T_{air}) and soil (T_s) temperature, respectively. GPP, R_E, R_S, and ET were estimated for the entire year with the use of continuous 20-min means of Q, T_{air}, and T_s. Annual NEE indicated that AL gained 536 g $CO_2 \cdot m^{-2}$, WB lost − 191 g $CO_2 \cdot m^{-2}$, CW was near equilibrium (− 14 g $CO_2 \cdot m^{-2}$), and VL exhibited considerable carbon accumulation (153 g $CO_2 \cdot m^{-2}$). The lower GPP values of the land-use types dominated by native species (CW and VL) compared to WB and AL were compensated by positive NEE values that were maintained during a longer growing season. As expected, VL and CW allocated a larger proportion of their carbon assimilates belowground. Non–growing-season R_E accounted for about 19% of annual R_E in all land-use types. The results of this landscape-level study suggest that carbon lost by cultivation of VLs is partially being restored when fields are left uncultivated, and that VLs are net sinks of carbon. Estimations of carbon balances have important management implications, such as estimation of ecosystem productivity and carbon credit certification.

Resumen

Un sistema de cámara cerrada móvil (CC) se utilizó para medir los flujos de carbono y agua en cuatro tipos comunes de uso de suelo en la ecorregión de la estepa de Kazajstán. Los usos de suelo representaron un cultivo (trigo o cebada, WB), tierras abandonadas (AL), triguillo crestado (CW) y tierras vírgenes (VL). Las mediciones se llevaron a cabo durante la estación de crecimiento del año 2002 en el norte de Kazajstán en tres sitios (bloques) distantes 15–20 km entre si. La CC permitió medir los componentes del flujo de carbono de intercambio neto del ecosistema (NEE), la respiración ecosistémica (R_E) y la respiración de suelo (R_S), junto con la evapotranspiración (ET). Se utilizó análisis de regresión no-lineal para modelar la producción primaria bruta (GPP) y ET en función de la radiación fotosintéticamente activa (Q); R_E y R_S se modelaron a partir de la temperatura del aire (T_{air}) y del suelo (T_s), respectivamente. Los GPP, R_E, R_S, y ET fueron estimados para el año completo usando los promedios continuos de 20 minutos de Q, T_{air} y T_s. El NEE anual mostró que AL ganó 536 g $CO_2 \cdot m^{-2}$, mientras que el WB emitió − 191 g $CO_2 \cdot m^{-2}$, el CW estaba cerca del equilibrio (− 14 g $CO_2 \cdot m^{-2}$), y la VL exhibió una acumulación de carbono considerable (153 g $CO_2 \cdot m^{-2}$). Los valores de GPP más bajos de los tipos de uso de suelos dominados por especies nativas (CW y VL) comparados con WB y AL fueron compensados por valores positivos de NEE, los cuales se mantuvieron durante una estación de crecimiento más prolongada. Tal como se esperaba, VL y CW destinaron una mayor proporción de sus carbonos asimilados debajo de la superficie del suelo. La R_E de la estación de receso representó un 19% de la R_E anual en todos los usos de suelo. Los resultados de este estudio a nivel de paisaje sugieren que el carbono perdido al momento de cultivar las tierras vírgenes está siendo parcialmente restaurado cuando los campos se dejan sin cultivar, y esas tierras vírgenes son sumideros netos de carbono. Las estimaciones de los balances de carbono tienen implicaciones importantes de manejo, tales como la estimación de la productividad del ecosistema y la certificación de crédito de carbono.

Key Words: abandoned fields, Kazakh steppe, net ecosystem exchange, nonlinear modeling, water-use efficiency, wheat

Research was funded by the Global Livestock Collaborative Research Support Program, Grant PCE-G-00-98-00036-00 from the US Agency for International Development. J.P.-Q. was funded by scholarships from the University of California–Davis.

The opinions expressed herein are those of the authors and do not necessarily reflect the views of the US Agency for International Development.

This publication was made possible through support provided to the Global Livestock Collaborative Research Support Program by the Office of Agriculture, Bureau for Economic Growth, Agriculture and Trade, United States Agency for International Development under terms of Grant No. PCE-G-00-98-00036-00. The opinions expressed herein are those of the author(s) and do not necessarily reflect the views of the USAID.

At the time of the research, Perez-Quezada was Research Assistant, Dept of Plant Sciences, University of California Davis, Davis, CA 95616, USA.

Correspondence: Jorge Perez-Quezada, Departamento de Ciencias Ambientales y Recursos Naturales Renovables, Universidad de Chile, Casilla 1004, Santiago, Chile. Email: jorgepq@uchile.cl

Manuscript received 14 April 2008; manuscript accepted 16 November 2008.

INTRODUCTION

Studies concerning the role of grasslands in the global carbon balance are relatively recent (Schuman et al. 2002). Grasslands are estimated to represent as much as 20% or more of total terrestrial production and may already be an annual carbon sink of 0.5 Pg (Scurlock and Hall 1998). Schimel et al. (2001) showed that most of the carbon sink is located in extratropical land areas of the northern hemisphere (lat > 30°N) with similar uptake rates in North America and Eurasia. Grasslands cover 40% of the Earth's surface (World Resources Institute 2000), and within this area, 17% are composed of the vast rangelands of Asia (excluding Russia and the Middle East). The Kazakh steppe ecoregion represents an area of 80.8 million ha that ranges from about lat 49°N to 54.5°N and from long 51°E to 83°E (Olson et al. 2001).

Northern Kazakhstan, similar to other areas in central and east Asia, has experienced major land-use changes during the last century, starting with the change from a mainly nomadic pastoral system to sedentary agriculture, which was promoted by the former Soviet Union (Chuluun and Ojima 2002). During the 1950s, Kazakhstan experienced a major land-cover change under Krushchev's "Virgin Lands" campaign, when about 15 million ha were plowed to produce spring wheat. These perturbations released a large quantity of carbon to the atmosphere (Chuluun and Ojima 2002). After the collapse of the Soviet Union in 1991, the wheat-growing area decreased by about 5 million ha until 1999, when wheat-growing areas began to increase (FAOSTAT 2008).

Much of the terrestrial carbon sink is due to land-use/management changes, including abandonment of agricultural lands (Schimel et al. 2001), which corresponds to a secondary succession process. Given the expansiveness of the Kazakh steppe ecoregion and its potential role in the global carbon cycle, it is critical to assess the capacity of various land uses in the Kazakh steppe to sequester carbon under current management conditions. Land uses that dominate this region include virgin land (VL) or typical steppe; pasture seeded with crested wheatgrass (*Agropyron cristatum subsp pectinatum* [M. Bieb.] Tzvelev; CW), which is cut and stored for hay each year; lands plowed to grow cereal crops (wheat and barley; WB); and abandoned land (AL) that previously grew crops, which have been abandoned for several years. This area is representative of about 39 million ha within the Kazakh steppe ecoregion (Olson et al. 2001), according to estimates by B. Wylie (2004; unpublished data using methodology by Lotsch et al. [2003] based on the analysis of MODIS satellite images [MODIS/Terra Land Cover Type 96-day L3 Global 1-km Integerized Sinusoidal (ISIN) Grid]).

Carbon has been shown to accumulate during the growing season on VL (Gilmanov et al. 2004a), but no measurements are available for WB, CW, or AL. A mobile closed chamber (CC) was used to measure carbon fluxes on the four land-use types. The objectives of this study were 1) to measure the instantaneous carbon flux components and water flux during the growing season on the four most representative land-use types in northern Kazakhstan, 2) to parameterize nonlinear models for predicting ecosystem fluxes of carbon and water, 3) to estimate seasonal and annual carbon and water balances, and 4) to analyze the influence of land-use change on regional carbon balance.

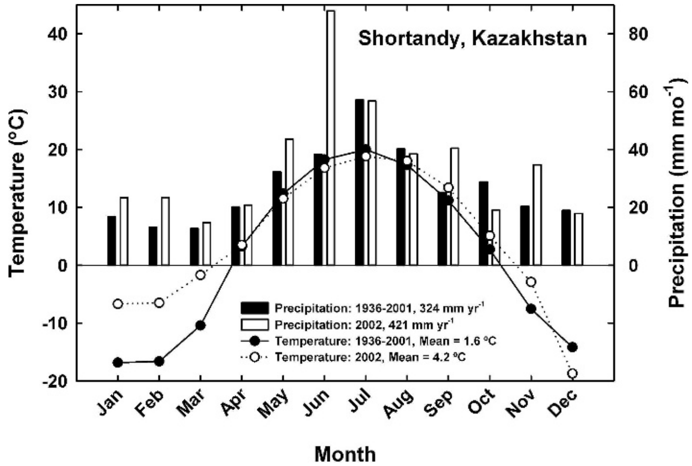

Figure 1. Mean long-term (1936–2001) and 2002 monthly precipitation and air temperature (Kazakh Research Institute of Grain Farming, meteorological station "Shortandy").

Because patterns of carbon capture and release are related to the life forms that grow in each land use, we hypothesized that 1) AL and WB would have high photosynthetic rates and their carbon allocation would be mainly aboveground; 2) CW and VL would have low assimilation rates and high belowground carbon allocation; and 3) carbon accumulation during the growing season would be in the order of WB > AL > VL > CW.

MATERIALS AND METHODS

Study Area and Sampling Design

The study was conducted on the Baraev Kazakh Research Institute of Grain Farming, located in northern Kazakhstan (lat 51°37′N, long 71°05′E), 367 m above sea level, 60 km north of Astana. The climate is cold, semiarid with 324 mm of average annual precipitation, 60% of which occurs between May and September (Fig. 1). Mean temperature for this same period was 15.8°C, whereas the annual mean temperature was 1.6°C.

Three locations about 15–20 km apart were used as blocks with all four land-use types represented in each block. These blocks were identified as Blocks 1, 3, and 4, as a part of a larger study. The study area is flat within and between blocks, with slopes generally < 3°. Selected research areas were large (> 50 ha), except for VL sites in blocks 3 and 4 (~ 5 ha and 2 ha, respectively), and all were within a radius of 1 km in each block. Within each field, two 1-m^2 plots were chosen as representative areas to measure CO_2 fluxes with the CC technique. There were 24 total plots (four land uses × three blocks × two plots per land-use type). The plots were separated from each other by about 90 m, and were at least 5 m from the field border (except for one VL plot), but generally were located about 200 m from the field border. Five measurement rotations of 1 d per block were completed from 28 May and 22 September 2002. Year 2002 was wetter (421 mm) and warmer (4.2°C) than the average year (Fig. 1).

Table 1. Abbreviations used.

AL	Abandoned land
CC	Closed-chamber system
CW	Crested wheatgrass
E_0	Temperature analogous to activation energy, K
ET	Evapotranspiration, mg $H_2O \cdot m^{-2} \cdot s^{-1}$ or mmol $H_2O \cdot m^{-2} \cdot s^{-1}$ or mm $H_2O \cdot yr^{-1}$
ET_{opt}	ET at "optimum" Q, mmol $H_2O \cdot m^{-2} \cdot s^{-1}$
F_c	Carbon flux, mg $CO_2 \cdot m^{-2} \cdot s^{-1}$
GPP	Gross primary production, mg $CO_2 \cdot m^{-2} \cdot s^{-1}$ or μmol $CO_2 \cdot m^{-2} \cdot s^{-1}$ or g $CO_2 \cdot m^{-2} \cdot yr^{-1}$
GPP_{opt}	GPP at "optimum" Q, μmol $CO_2 \cdot m^{-2} \cdot s^{-1}$
NEE	Net ecosystem exchange, mg $CO_2 \cdot m^{-2} \cdot s^{-1}$ or g $CO_2 \cdot m^{-2} \cdot yr^{-1}$
Q	Photosynthetically active radiation, μmol quantum $\cdot m^{-2} \cdot s^{-1}$
R_{10}	R_E at 10°C, μmol $CO_2 \cdot m^{-2} \cdot s^{-1}$
R_C	Canopy respiration, mg $CO_2 \cdot m^{-2} \cdot s^{-1}$
R_E	Ecosystem respiration, mg $CO_2 \cdot m^{-2} \cdot s^{-1}$ or μmol $CO_2 \cdot m^{-2} \cdot s^{-1}$ or g $CO_2 \cdot m^{-2} \cdot yr^{-1}$
R_S	Soil respiration mg $CO_2 \cdot m^{-2} \cdot s^{-1}$ or μmol $CO_2 \cdot m^{-2} \cdot s^{-1}$
SOC	Soil organic C, %
T_{air}	Air temperature, °C
T_s	Soil temperature, °C
VL	Virgin land
WB	Wheat-barley cropland
WUE	Water-use efficiency, g $CO_2 \cdot m^{-2} \cdot d^{-1} \cdot mm^{-1}$ H_2O
α	Initial slope of the rectangular hyperbolic curve, μmol $CO_2 \cdot$ mmol quantum^{-1} or mmol $H_2O \cdot$ mmol quantum^{-1}

The AL sites were dominated by Canada thistle (*Cirsium arvense* [L.] Scop.), field sowthistle (*Sonchus arvensis* L.), and shrub species from the genera *Matricaria* and *Artemisia*. The VL plots were dominated by Volga fescue (*Festuca valesiaca* Schleich. ex Gaudin), stipa (*Stipa capillata* L.), and shrubs (*Artemisia* spp.). The CW plots had a cover of $> 90\%$ of crested wheatgrass, and the WB plots had a cover of $> 90\%$ wheat (*Triticum aestivum* L.) or, in the case of Block 3, barley (*Hordeum vulgare* L.), respectively. The botanical nomenclature follows that of the Missouri Botanical Garden (Tropicos.org 2008).

Soils on the study sites are calcareous southern chernozems with interspersed solonetz–solonchaks complexes. The landscape is nearly level, with average slope generally less than 2%. Three soil samples (diameter = 6 cm) were taken to a depth of 4.5 cm during spring and late summer at each site to estimate bulk density, soil nitrogen, and organic carbon content. Soil carbon and nitrogen contents were measured with a Europa 20-20 continuous-flow isotope ratio mass spectrometer (PDZ Europa Ltd., Sandbach, United Kingdom), following combustion at 1 000°C in a Europa ANCA-GSL CN analyzer (PDZ Europa Ltd.). Before analysis, roots were removed and the soil sample was ball-milled for 12 h. Separation of the organic fraction of soil carbon was accomplished by the acid fumigation method of Harris et al. (2001), which eliminated inorganic carbonates by exposure to concentrated (12 M) HCl.

CO_2 Fluxes, Evapotranspiration, and Micrometeorological Measurements

Estimations of CO_2 fluxes (F_c, mg $CO_2 \cdot m^{-2} \cdot s^{-1}$; see Table 1 for the list of symbols and units), and evapotranspiration (ET, mg $H_2O \cdot m^{-2} \cdot s^{-1}$) were obtained with a CC system, which consisted of an LI-6200 portable gas-exchange system (LI-COR, Lincoln, NE) connected to a 1-m^3 canopy chamber modified after Held et al. (1990). The frames consisted of 1.2-cm aluminum angles, which were covered with Mylar film (0.05 mm thick). Three fans (40 100 $cm^3 \cdot s^{-1}$ each) mixed the air inside the chamber 10 s before and during the measurements to obtain a steady-state sample (i.e., linear decrease or increase in CO_2 and water-vapor concentration with time). The CC system also included sensors that measured photosynthetically active radiation (Q; quantum sensor, model LI-190S-1, LI-COR), air temperature (T_{air}; thermocouple), and air relative humidity (Vaisala HUMICAP®, Helsinki, Finland).

The CC operated as a closed system with air circulating through the chamber and the infrared gas analyzer (IRGA). The F_c was calculated from the slope generated by the decreasing (photosynthesis) or increasing (respiration) concentration of CO_2 inside the chamber versus time. Similarly, ET was calculated from the increasing concentration of water-vapor concentration inside the chamber. An angled (90°) 1-m^2 metal frame was installed at each plot. This 1-m^2 frame provided a flat surface with which the bottom of the CC was tightly sealed as a layer of closed-cell foam affixed to the bottom of the CC prevented the air from leaving or entering the CC. Setting the CC on top of the 1-m^2 plot-frame, executing the gas exchange measurement, and removing the CC took about 2 min per plot. Additionally, a soil respiration collar (polyvinyl chloride cylinder, 5 cm high by 10.4-cm diameter; inside area = 85 cm^2) was installed inside the 1-m^2 plot to measure soil respiration (R_S). Plants growing inside the soil respiration collar were removed so that R_S measurements represented belowground CO_2 efflux.

Measurements with the CC during daylight periods were used to quantify net ecosystem exchange (NEE). Ecosystem

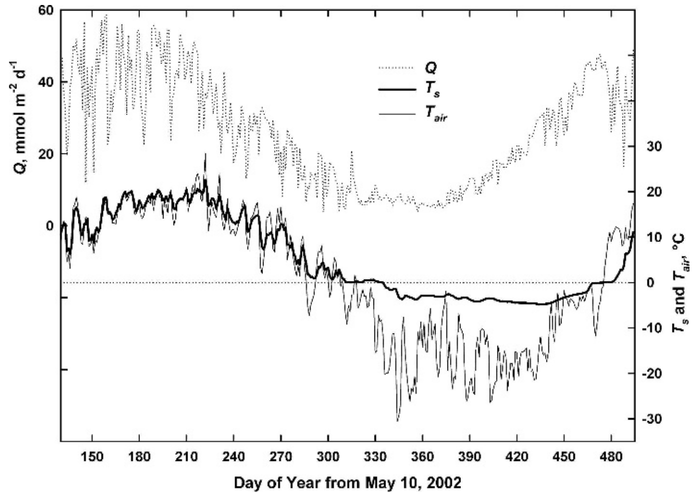

Figure 2. Daily cumulative Q (left axis) and mean T_s, T_{air} (right axis) from continuous measurements taken at the AL site of block 1. Data from Julian day (DOY) 130 to 365 are from 2002, and data from DOY 366 to 494 are from 2003. See Table 1 for definitions of abbreviations.

respiration (R_E) was obtained by covering the chamber with an opaque material to stop photosynthesis and photorespiration instantaneously. These "dark" measurements were done immediately after covering the chamber to avoid dramatic changes in environmental conditions. Between the light and dark measurements, the chamber was removed from the plot for about 1 min. The fans continued to operate during this period to ventilate the chamber and equilibrate conditions inside and outside the chamber. R_S was measured with the use of a soil respiration chamber (model 6000-09, LI-COR) and the LI-6200 system. Soil temperature (T_s) at a 10-cm soil depth was measured with a soil temperature probe (model 6000-09TC, LI-COR).

One day of CC measurements in one block consisted of four to six visits at each plot, depending on the available logistics and manpower. Estimates of NEE, R_E, R_S, and ET were obtained each time a plot was sampled. Measurements began at 0800 hours, and the last set of measurements was taken after sunset. The IRGA of the LI-6200 system was calibrated for zero and span (400 ppm) values of CO_2 concentration, prior to each day of measurements.

Hooper et al. (2002) found that the F_c data obtained with a LI-6200 required correction when chamber vapor pressure increased $> 0.3\ mb \cdot s^{-1}$. This correction was applied to our data with the use of the equation given by LI-COR (2001). Quality control of the data was performed following the recommendations of the manufacturer (LI-COR 1987), which eliminated 185 (11.7%) measurements, and left 1 403 data points for analyses.

During the daylight hours, positive values of NEE represented CO_2 uptake by the ecosystem, whereas negative values denoted CO_2 efflux (respiration) from the ecosystem. Gross primary production (GPP) was estimated during the day as

$$GPP = NEE + R_E. \quad [1]$$

Canopy respiration (R_C) was calculated as $R_E - R_S$. R_S in our case represents the components of soil respiration (plant-derived and soil organic matter–derived, including microbial respiration of dead plant residues laying on the soil surface). We used positive values of respiration and its components in our modeling and data analyses.

The number of days to complete the flux measurements from the first to the last block were 8, 16, 6, 10, and 11 d for each of the five sampling periods, respectively. Thus, the mean Julian day (DOY) of each of the five sampling periods was 152 (early-June), 168 (mid-June), 191 (mid-July), 230 (mid-August), and 260 (mid-September). Values of T_s, T_{air}, and Q were continuously measured in the AL site of block 1 between DOY 130 in 2002 and DOY 129 in 2003 (Fig. 2), with the use of two sets of soil temperature probes (model TCAV, Campbell Scientific Inc., Logan, UT), a platinum resistance temperature detector (model HMP45C, Campbell Scientific), and a quantum sensor (model LI190SB, LI-COR).

Even though we took the precautions to make the CC measurements as short as possible and ventilated the chamber between measurements, the well-known chamber effect was evident in our data. This effect consisted of a higher T_{air} inside the chamber (average difference of 2.2°C) than outside T_{air}, by sensors installed in nearby eddy covariance stations (data not shown). Similarly, the Q level measured inside the chamber was lower than outside because of the effect of the Mylar film of the chamber. We did not make any adjustment for the differences between the CC and micrometeorological (BREB) data during model parameterizations and simulations, because our main interest was in making comparisons in fluxes between land-use types, and a unique set of micrometeorological data was used for predictions.

Modeling Carbon and Water Fluxes

Flux measurements were pooled into groups according to particular agroecosystem–period combination, which resulted in 20 data sets (four agroecosystem × five measurement periods). Within a measurement period for each land use, a data set consisted of three blocks or replicates × two plots × i measurements (i.e., the numbers of measurements within a measurement period were not the same). A data set for each agroecosystem–period combination consisted of four subsets or types of flux measurements (GPP, R_E, R_S, and ET).

GPP was modeled with the use of the light-response equation modified from Smith (1938) as modified by Falge et al. (2001):

$$GPP = \frac{\alpha \cdot Q \cdot GPP_{opt}}{\sqrt{(GPP_{opt})^2 + (\alpha \cdot Q)^2}}, \quad [2]$$

where α is the initial slope of the rectangular hyperbolic curve or the ecosystem quantum yield ($\mu mol\ CO_2 \cdot \mu mol\ quantum^{-1}$); and GPP_{opt} is the GPP ($\mu mol\ CO_2 \cdot m^{-2} \cdot s^{-1}$) at "optimum" photosynthetically active radiation (Q, $\mu mol\ quantum \cdot m^{-2} \cdot s^{-1}$). This model was selected among others tested because it gave the best overall fit of the data. We used only one single model to allow us to compare the parameters between the different land uses and periods.

We used the exponential equation from Lloyd and Taylor (1994) to model ecosystem respiration (R_E) as applied by Reichstein et al. (2005):

Table 2. Soil characteristics for each land-use type in the top 15-cm soil layer. Values are mean ± standard error. Values within a column followed by the same letter are not statistically different ($P < 0.05$) as indicated by the Tukey–Kramer test.

Land use	Bulk density ($kg \cdot m^{-3}$)	Organic carbon ($kg \cdot m^{-2} \cdot 15\ cm^{-1}$)	Total nitrogen ($g \cdot m^{-2} \cdot 15\ cm^{-1}$)
Wheat/barley	963 ± 26 b	3.52 ± 0.22 b	341 ± 19 b
Abandoned land	1 048 ± 26 a	3.57 ± 0.22 b	343 ± 19 b
Crested wheatgrass	1 103 ± 27 a	4.17 ± 0.22 ab	404 ± 19 ab
Virgin land	968 ± 27 b	4.90 ± 0.22 a	467 ± 19 a

$$R_E = R_{10} \cdot \exp\{E_0 \cdot [1/(T_{ref} - T_0) - 1/(T - T_0)]\}, \quad [3]$$

where R_{10} is the R_E at 10°C (μmol $CO_2 \cdot m^{-2} \cdot s^{-1}$); E_0 is the temperature (K) analogous to activation energy; T_{ref} is the reference temperature = 283.15 K (10°C); T_0 is a constant at 227.13 K (− 46.02°C); and T is the temperature (K) of the darkened canopy chamber. R_S was modeled with the use of Equation 3, but with T as the temperature (K) from the soil probe during soil chamber measurement.

The same light-response equation as in GPP was used to model water-vapor flux or evapotranspiration (ET, mmol $H_2O \cdot m^{-2} \cdot s^{-1}$):

$$ET = \frac{\alpha \cdot Q \cdot ET_{opt}}{\sqrt{(ET_{opt})^2 + (\alpha \cdot Q)^2}}, \quad [4]$$

where α is the initial slope of the rectangular hyperbolic curve (mmol $H_2O \cdot$ mmol $quantum^{-1}$) and ET_{opt} is evapotranspiration (mmol $H_2O \cdot m^{-2} \cdot s^{-1}$) at "optimum" Q (mmol quantum $\cdot m^{-2} \cdot s^{-1}$). The nonlinear regression (NLIN) procedure in SAS (SAS 2001) was used to parameterize the models for GPP, R_E, R_S, and ET by statistically analyzing each data set pooled according to agroecosystem–measurement period combination. Thus, a total of 80 models (i.e., four agroecosystems × five measurement periods × four flux types) were parameterized. The goodness of fit of the nonlinear models was calculated as the ratio between sum of squares due to regression (SSR) and the total sum of squares (SST):

$$R^2 = \frac{SSR}{SST}. \quad [5]$$

The four types of fluxes were estimated on a 20-min basis for the entire growing season, with the use of the nonlinear models (Equations 2–4) and the continuous micrometeorological data (Fig. 2). Modeled NEE was calculated from the modeled values of GPP and R_E with the use of Equation 1. R_E for the nongrowing season was modeled with the use of the parameters of early June and mid-September for each land use.

Water-use efficiency (WUE) was calculated following Emmerich (2007), as the value of the regression slope for daily daytime NEE (g $CO_2 \cdot m^{-2} \cdot d^{-1}$) vs. daily daytime ET (mm $H_2O \cdot d^{-1}$), for all the days of the growing season, based on the modeled 20-min fluxes.

RESULTS

Soil Characteristics

Values of soil bulk density for all land-use types were below 1 300 $kg \cdot m^{-3}$ (Table 2), which is considered a typical value for agricultural soils (Loomis and Connor 1992). Bulk density values for CW and AL were significantly higher (1 100 and 1 050 $kg \cdot m^{-3}$, respectively) than those for VL and WB (both about 965 $kg \cdot m^{-3}$).

Soil organic carbon (SOC) and nitrogen content from samples collected in spring were not significantly different (paired t test) from those collected in late summer ($P = 0.63$ and 0.24 for SOC and total nitrogen, respectively). Consequently, data for these two periods were pooled for further analyses. The levels of SOC and nitrogen content were significantly higher in VL compared to AL and WB land-use types.

Instantaneous CO_2 and Water Fluxes

Mean instantaneous CO_2 and evapotranspiration fluxes are shown in Figure 3. NEE reached its maximum value about DOY 152 for VL (0.12 mg $CO_2 \cdot m \cdot s^{-1}$) and CW (0.14 mg $CO_2 \cdot m^{-2} \cdot s^{-1}$), and later (DOY = 168) for AL (0.31 mg $CO_2 \cdot m^{-2} \cdot s^{-1}$) and WB (DOY = 191, 0.27 mg $CO_2 \cdot m^{-2} \cdot s^{-1}$). GPP reached a maximum in mid-July (DOY 191) with WB–AL exhibiting the highest levels (about 0.78 mg $CO_2 \cdot m^{-2} \cdot s^{-1}$; Fig. 3). Maximum GPP levels for CW and VL were about 0.44 mg $\cdot m^{-2} \cdot s^{-1}$ in mid-June and mid-July.

Daily average respiration components and ET achieved their maxima in mid-July (DOY = 191) for all land uses (Fig. 3). Maximum mean values of R_E were 0.52 mg $CO_2 \cdot m^{-2} \cdot s^{-1}$ for AL and 0.46 mg $CO_2 \cdot m^{-2} \cdot s^{-1}$ for WB, 0.40 mg $CO_2 \cdot m^{-2} \cdot s^{-1}$ for VL, and 0.37 mg $CO_2 \cdot m^{-2} \cdot s^{-1}$ for CW. R_S was higher than R_C except between mid-June and mid-August in AL, and in mid-August in CW and WB. Maxima for ET were quite similar among land-use types with slightly higher values for CW and WB (0.18 and 0.19 mg $H_2O \cdot m^{-2} \cdot s^{-1}$, respectively) compared to AL and WB (0.15 and 0.16 mg $H_2O \cdot m^{-2} \cdot s^{-1}$, respectively).

Nonlinear Modeling of Instantaneous Fluxes

The nonlinear models (Equations 2–4) represented the variation in carbon and water fluxes quite well for the different land-use types during the growing season (Fig. 4). The parameters for the nonlinear models are presented in Table 3. Values of maximum assimilation rates (i.e., optimum GPP, GPP_{opt}) were higher for WB and AL (~ 26.6 μmol $CO_2 \cdot m^{-2} \cdot s^{-1}$) than CW and VL (14.0 and 15.2 μmol $CO_2 \cdot m^{-2} \cdot s^{-1}$, respectively). At the beginning of the growing season, maximum values of R_E at 10°C (R_{10}, μmol $CO_2 \cdot m^{-2} \cdot s^{-1}$) were similar in CW and VL (3.35 and 3.42 μmol $CO_2 \cdot m^{-2} \cdot s^{-1}$, respectively), whereas maximum values in AL and WB were reached in mid-July (3.85 and 4.2 μmol $CO_2 \cdot m^{-2} \cdot s^{-1}$, respectively). Results showed that the nonlinear models fit the data well, with R^2 values ranging between 0.65 and 0.99 (Table 3), being generally higher for CW and VL. The lower minimum R^2 values for WB and AL were due to the difficulty in modeling the data for mid-August and mid-September in AL and for early-June and mid-September in WB, which were the periods with lowest assimilation rates in these two land-use types. Values of maximum evapotranspiration rates (i.e., optimum ET, ET_{opt})

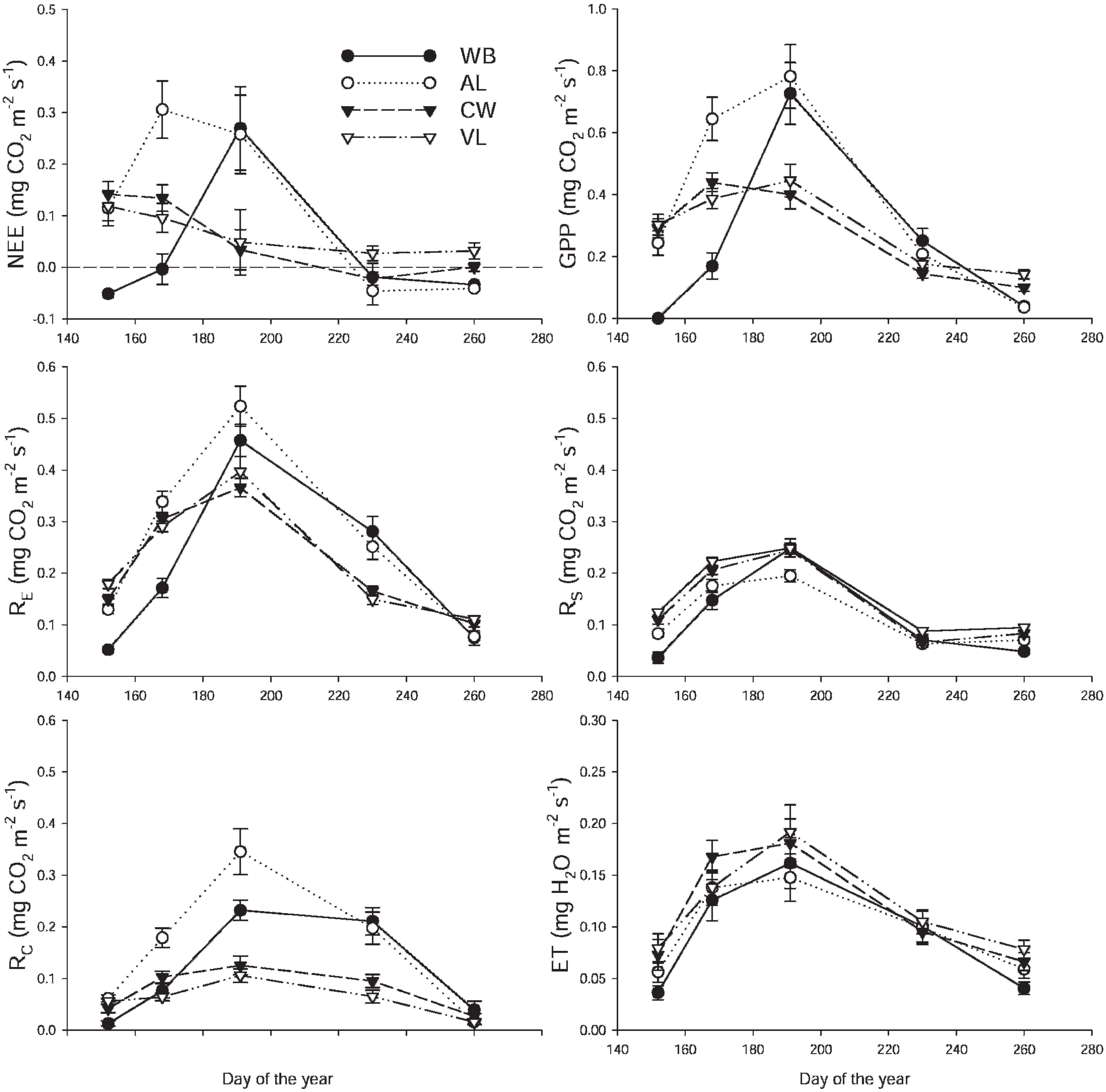

Figure 3. Net ecosystem exchange (NEE), gross primary production (GPP), ecosystem respiration (R_E), soil respiration (R_S), canopy respiration (R_C), and evapotranspiration (ET) for wheat/barley (WB), abandoned land (AL), crested wheatgrass (CW), and virgin land (VL), at the midpoint Julian day of each sampling period. Values are mean ± standard error.

were higher for CW and VL (~ 10.0 mmol $H_2O \cdot m^{-2} \cdot s^{-1}$) than WB and AL (6.0 mmol $H_2O \cdot m^{-2} \cdot s^{-1}$, respectively).

Seasonal Fluxes and Water-Use Efficiency

The growing season and annual fluxes obtained with the use of the nonlinear models with the continuous 20-min micrometeorological data are presented in Table 4. AL had the highest GPP value (3 445 g $CO_2 \cdot m^{-2}$), followed by VL (2 521 g $CO_2 \cdot m^{-2}$), WB (2 315 g $CO_2 \cdot m^{-2}$), and CW 2 240 (g $CO_2 \cdot m^{-2}$). Annual R_E was higher than the CO_2 accumulated for WB and CW land-use types, which resulted in an annual net loss of carbon to the atmosphere (NEE = − 191 and − 14 g $CO_2 \cdot m^{-2}$, respectively). AL exhibited the highest annual R_E and greatest annual positive net carbon fixation (NEE = 536 g $CO_2 \cdot m^{-2}$), whereas VL had a low but positive NEE value (153 g $CO_2 \cdot m^{-2}$). Values of ET during the growing season were highest for VL (362 mm), followed by CW, AL, and WB (ET = 334 mm, 291 mm, and 260 mm, respectively).

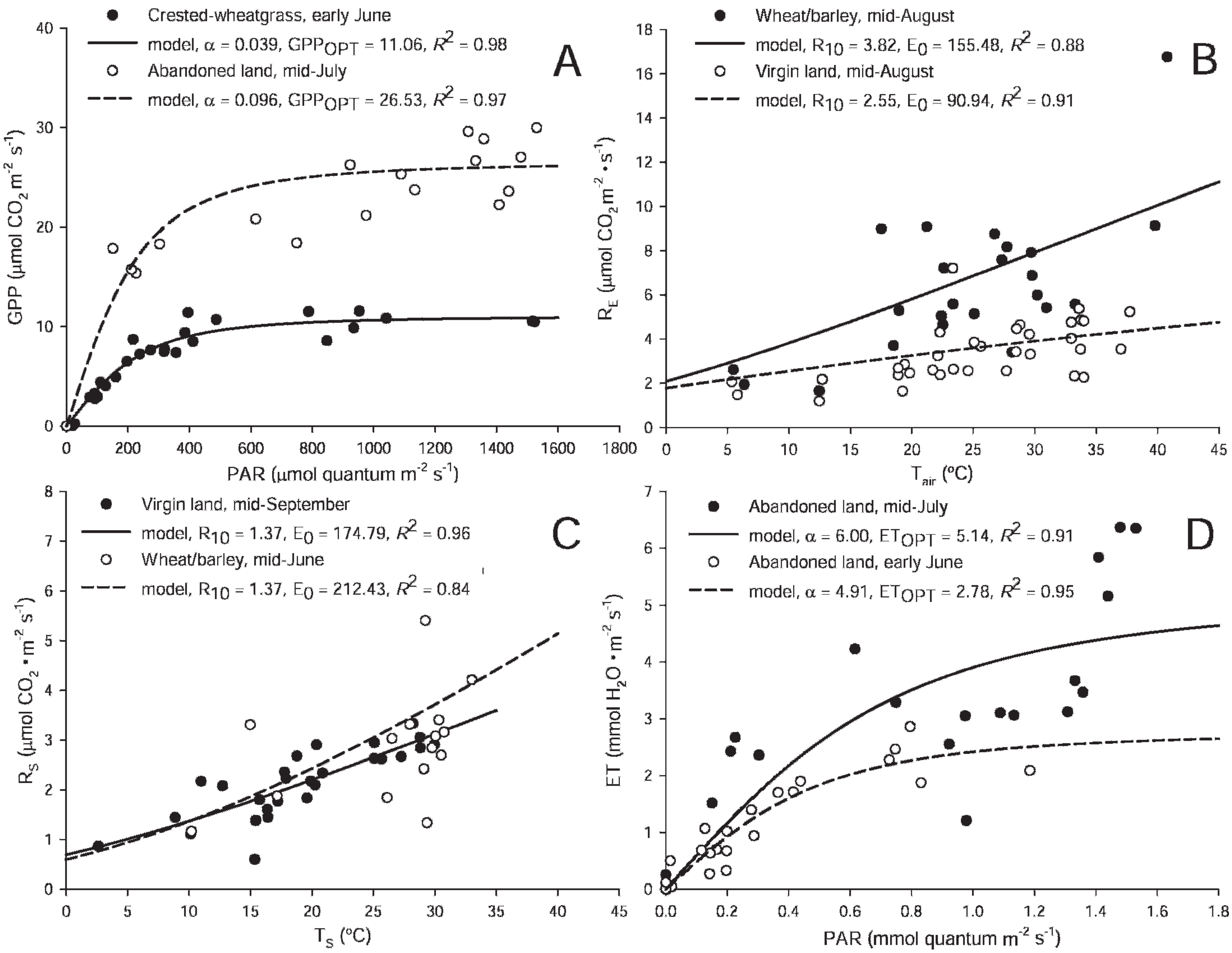

Figure 4. Nonlinear models (Equations 2–4) fitted to **A**, gross primary production (GPP); **B**, ecosystem respiration (R_E); **C**, soil respiration (R_S); and **D**, evapotranspiration (ET). See Table 1 for definitions of abbreviations. Parameters of models are detailed in Table 3.

Mean values of WUE for the growing season were similar for the CW and VL land-use types (3.8 and 4.0 g $CO_2 \cdot m^{-2} \cdot mm^{-1}$ H_2O, respectively) and were considerably lower than those for WB and AL (8.8 and 10.8 g $CO_2 \cdot m^{-2} \cdot mm^{-1}$ H_2O, respectively; Fig. 5).

DISCUSSION

The CC technique is generally recommended for use in estimating the spatial variability of carbon fluxes (F_c) within a site, which cannot be assessed by tower techniques (Laine et al. 2006; Risch and Frank 2006), or to separate the components of F_c (Risch and Frank 2006; Ohkubo et al. 2007). In our study, we used the CC system to sample F_c components in four land-use types. Because we sampled land uses in three different blocks, we were able to capture the spatial variability present at the landscape level, which likely increased the representativeness of our modeled parameters. This approach is more cost-effective than using stationary tower systems to monitor F_c.

Our approach of estimating GPP from estimates of NEE and R_E, which was done independently within a few minutes, differs from more traditional approaches where R_E is estimated from light-response models of NEE or from models of R_E using nighttime NEE data, when NEE = R_E. The approach we used has the advantage that GPP is more closely related to light levels (Q) than NEE, which facilitates fitting the data to light-response models. The potential bias caused by using R_E data from one period of the day to model whole-day R_E (as is the case in the traditional approach mentioned above), may have been a problem in our study also because nighttime R_E was represented only by one measurement after nightfall because of logistic restrictions. The same potential problem exists for the winter period when parameters of R_E models were fit using data from early June and mid-September for each land use. This may have resulted in somewhat higher estimates of average daily R_E for the nongrowing season (AL = 3.03, VL = 2.37, CW = 2.19, and WB = 1.74 g $CO_2 \cdot m^{-2} \cdot d^{-1}$) compared to the values summarized by Gilmanov et al. (2004b) from several studies for tundra (0.23–0.6 g $CO_2 \cdot m^{-2} \cdot d^{-1}$), sagebrush steppe (0.68–1.31 g $CO_2 \cdot m^{-2} \cdot d^{-1}$), mixed prairie (1.7–2.03 g $CO_2 \cdot m^{-2} \cdot d^{-1}$), and tallgrass prairie (2.25–3.5 g $CO_2 \cdot m^{-2} \cdot d^{-1}$).

Table 3. Parameters and coefficient of determination of nonlinear models (Equations 2–4) for carbon and water fluxes.[1]

Land use	Parameters					
	min α	max α	min GPP_{opt}	max GPP_{opt}	min R^2	max R^2
Gross primary production						
Abandoned land	0.026	0.096	1.09	26.53	0.65	0.98
Crested wheatgrass	0.019	0.040	3.31	14.04	0.93	0.99
Virgin land	0.019	0.042	5.17	15.24	0.94	0.98
Wheat/barley	0.003	0.066	2.24	26.64	0.43	0.99
R_E						
	min R_{10}	max R_{10}	min E_0	max E_0	min R^2	max R^2
Abandoned land	1.42	3.85	114.79	285.38	0.78	0.98
Crested wheatgrass	1.48	3.35	151.13	365.44	0.95	0.98
Virgin land	1.28	3.42	90.94	315.80	0.92	0.98
Wheat/barley	1.13	4.20	155.48	320.40	0.73	0.98
R_S						
	min R_{10}	max R_{10}	min E_0	max E_0	min R^2	max R^2
Abandoned land	1.04	2.92	77.46	154.43	0.73	0.94
Crested wheatgrass	1.12	4.48	25.71	190.03	0.87	0.95
Virgin land	1.32	3.21	106.25	174.79	0.94	0.97
Wheat/barley	0.84	3.94	23.43	316.50	0.84	0.99
Evapotranspiration						
	min α	max α	min ET_{opt}	max ET_{opt}	min R^2	max R^2
Abandoned land	3.29	6.00	2.78	6.33	0.89	0.96
Crested wheatgrass	3.74	5.85	3.18	9.11	0.92	0.97
Virgin land	3.69	5.58	3.28	11.68	0.92	0.97
Wheat/barley	2.48	7.51	1.82	5.68	0.83	0.97

[1] GPP_{opt} indicates gross primary production at "optimum" Q; R_E, ecosystem respiration; R_{10}, R_E at 10°C; E_0, temperature analogous to activation energy, K; R_S, soil respiration; and ET_{opt}, evapotranspiration at "optimum" Q.

Fluxes of water and carbon are tightly coupled, and thus it seems intuitive that similar environmental factors must have driven ET and GPP during daytime (i.e., $Q > 0$). In the present study, we used a relatively simple model with Q as the driving variable to estimate ET. The advantage of our approach is its simplicity compared to the commonly used Penman–Monteith equation, which requires knowing the canopy resistance to water-vapor flux. However, our calculations could underestimate ET because our model assumes that nighttime ET (i.e., $Q = 0$) is zero, which may not be true sometimes. In addition, some lack of fit was observed also in some periods (e.g., Fig. 4D), probably due to the fact that data came from different blocks, or because, as observed by Irmak et al. (2008), Q is more related to stomatal resistance at lower levels of radiation (0–0.25 $mmol \cdot m^{-2} \cdot d^{-1}$).

Mean instantaneous fluxes during the growing season exhibited very similar patterns for CW and VL (Fig. 3), which was expected because crested wheatgrass naturally occurs in northern Kazakhstan and was similar to the life forms of the native steppe vegetation. The main differences between WB and AL occurred in early-June and mid-June, when WB was initiating growth and AL had already accumulated considerable biomass. Flux patterns for WB were very similar to AL starting in mid-July.

As expected, WB exhibited the highest photosynthetic rates (GPP in Fig. 3 and maximum GPP_{opt} in Table 3), which were similar to those for AL and much higher than for CW and VL. However, the latter two land-use types had higher GPP in early June and mid-September, which is indicative of their longer growing season. That is, vegetation in WB and AL grew more

Table 4. Gross primary production (GPP, g $CO_2 \cdot m^{-2}$), ecosystem respiration (R_E, g $CO_2 \cdot m^{-2}$), net ecosystem exchange (NEE, g $CO_2 \cdot m^{-2}$), and evapotranspiration (ET, mm) for the growing season, nongrowing season, and entire year as modeled from closed chamber measurements for four land-use types in northern Kazakhstan. NEE was calculated as GPP − R_E.

Period	Wheat/barley					Abandoned land					Crested wheatgrass					Virgin land				
	GPP	R_E	R_S[1]	NEE	ET	GPP	R_E	R_S	NEE	ET	GPP	R_E	R_S	NEE	ET	GPP	R_E	R_S	NEE	ET
Grow[2]	2 315	2 082	1 057	233	260	3 445	2 341	1 137	1 104	291	2 240	1 831	1 448	409	334	2 521	1 898	1 580	623	362
Nongrow	0	424	284	− 424		0	568	433	− 568		0	423	336	− 423		0	470	441	− 470	
Annual	2 315	2 506	1 341	− 191		3 445	2 909	1 570	536		2 240	2 254	1 784	− 14		2 521	2 368	2 021	153	

[1] R_S indicates soil respiration.
[2] Growing season for wheat/barley was Julian day (DOY) 150–270, abandoned land was DOY 122–270, and crested wheatgrass and virgin land was DOY 121–289.

vigorously but senesced more rapidly than vegetation in CW and VL. R_E followed the trend of GPP for all land-use types but was always less than GPP, except in early June for WB and in mid-August and mid-September for WB and AL (Fig. 3). This implied that NEE was negative in these periods for WB-AL and always positive in VL-CW.

The maximum instantaneous NEE values observed for CW and VL (0.36 and 0.43 mg $CO_2 \cdot m^{-2} \cdot s^{-1}$) were higher than the values reported by Zhang et al. (2007) for the steppe in semiarid Inner Mongolia (0.29 mg $CO_2 \cdot m^{-2} \cdot s^{-1}$). The values we observed in AL and WB (0.91 and 1.02 mg $CO_2 \cdot m^{-2} \cdot s^{-1}$, respectively) were also higher than the value reported by Zhang et al. (2007) for a mixed cropland (0.59 mg $CO_2 \cdot m^{-2} \cdot s^{-1}$).

The annual balance of R_E was in the order AL > WB > VL > CW, from which nongrowing season R_E represented a relatively similar proportion for all land-use types (17% for WB, 19% for CW, and 20% for AL and VL; Table 4). Because of extremely low temperatures and lack of snow removal on the roads in our study area, it was not possible to conduct CC measurements under snow-cover conditions during the winter. Therefore, our estimates of wintertime R_E should be interpreted with caution. In terms of the proportion that wintertime R_E represents of the entire year, our estimates are higher than those reported for sagebrush steppe (11–12%; Gilmanov et al. 2004b) and Japanese cool-temperate forests (Mariko et al. 2000).

Both annual and growing season R_S were in the order VL > CW > AL > WB. The proportion that annual R_S represented of annual R_E was 83% for VL, 79% for CW, 51% for WB, and 49% for AL (Table 4). These patterns of higher R_S values and R_S representing a greater proportion of R_E for VL and CW may be because these systems allocate a high proportion of their carbon to belowground structures. This may be because the dominant species in these land-use types are perennial grasses. Correspondingly, because WB and AL are dominated by annual species, only about half of the carbon is allocated to belowground structures and the other half is allocated to R_C. These higher values of R_S for VL and CW are consistent with the higher SOC and nitrogen contents in these land-use types (Table 2). The difference in SOC between VL and WB was on average about 1.4 $kg \cdot m^{-2} \cdot 15\ cm^{-1}$. A higher (but nonsignificant) SOC was observed in AL compared to WB, which suggests that carbon lost by cultivation is being restored in the soil after abandonment. The difference in nitrogen content between VL and WB (126 $g \cdot m^{-2} \cdot 15\ cm^{-1}$) also suggests that nitrogen was lost in the cultivation of VL. However, these differences may not be solely due to management practices. For example, the high bulk density values in CW may be partially explained by the typical establishment of crested wheatgrass on soils with low organic matter content (K. Akshalov, personal communication, December 2007). The lower bulk density values of AL and WB compared to CW may be due to soil cultivation.

The higher ET rates observed for VL and CW compared to AL and WB (Table 3) made the total ET during the growing season follow in the order VL > CW > AL > WB (Table 4). When daily daytime CO_2 uptake was divided by daily daytime ET, values of WUE were AL > WB > VL > CW (Fig. 5). The values of WUE for VL and CW (about 3.8 g $CO_2 \cdot m^{-2} \cdot mm^{-1}$ H_2O) are high compared to the values reported by Emmerich (2007), who found that WUE during the growing season was 1.74 g $CO_2 \cdot m^{-2} \cdot mm^{-1}$ H_2O for a desert grassland site in southeastern Arizona but was 1.28 g $CO_2 \cdot m^{-2} \cdot mm^{-1}$ H_2O for a desert shrubland site. Our estimates of WUE for WB and AL (8.76 and 10.38 g $CO_2 \cdot m^{-2} \cdot mm^{-1}$ H_2O) are also higher than the WUE values of 5.5–7.62 g $CO_2 \cdot m^{-2} \cdot mm^{-1}$ H_2O reported for winter wheat (Zhao et al. 2007).

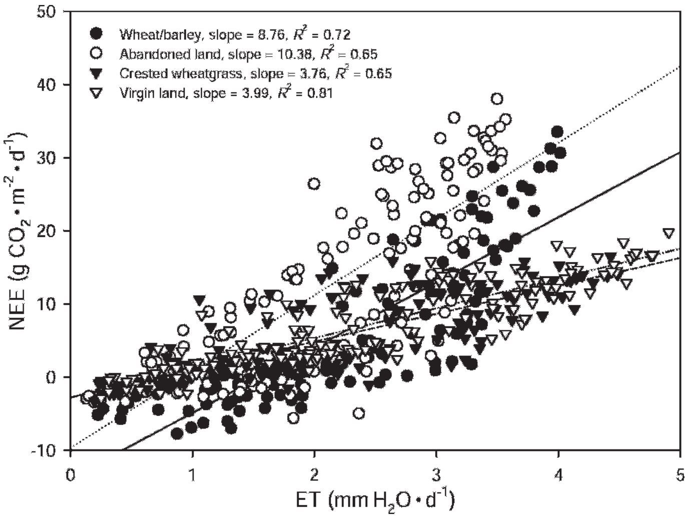

Figure 5. Daytime net ecosystem exchange (NEE) and evapotranspiration (ET) during the growing season. Lines are linear models for wheat-barley cropland (solid), abandoned land (dotted), crested wheatgrass (dashed), and virgin land (dashed-dotted).

The growing season and annual NEE balance was in the order AL > VL > CW > WB (Table 4). This was probably due to the later initiation of growth for WB (about DOY 150) compared to AL, VL, and CW, which already exhibited considerable biomass accumulation by that time. Furthermore, during the period immediately before and after the sowing of the wheat and barley, WB exhibited high values of R_E that resulted in considerable CO_2 loss. The lower maximum CO_2 accumulation rates for VL and CW were compensated by their longer growth period.

Table 5 shows a compilation of estimates of GPP, R_E, and NEE for various ecosystems dominated by short-statured vegetation. The NEE value for the growing season in VL (623 g $CO_2 \cdot m^{-2}$) is quite close to the maximum value reported by Gilmanov et al. (2004a; range of 328–635 g $CO_2 \cdot m^{-2}$), who sampled the VL site of Block 1 during four growing seasons (1998–2001). Their maximum value of GPP was 1 957 g $CO_2 \cdot m^{-2}$ and for R_E was 1 322 g $CO_2 \cdot m^{-2}$. The higher values observed in our current study (Table 4) may be due to the greater precipitation and warmer temperatures exhibited during 2002 compared to the previous years of measurement (Fig. 1). The estimates of annual NEE for the four land-use types in our current study fall within the observed values for similar land-use types (Table 5).

Changes in land use as driven by market or government decisions can have important effects on regional carbon balance. For example, if the difference in annual carbon balance between WB and AL obtained in our current study (727 g $CO_2 \cdot m^{-2} \cdot yr^{-1}$) is multiplied by the maximum

Table 5. Gross primary production (GPP), ecosystem respiration (R_E), and net ecosystem CO_2 exchange (NEE) in various ecosystems dominated by short-statured vegetation (after Gilmanov et al. 2006).

Ecosystem, site	GPP g $CO_2 \cdot m^{-2} \cdot$ period^{-1}	R_E g $CO_2 \cdot m^{-2} \cdot$ period^{-1}	NEE g $CO_2 \cdot m^{-2} \cdot$ period^{-1}	Source	Period, days
Northern mixed prairie, Miles City, MT, USA	913–1 239	1 130–1437	− 198 to − 217	Gilmanov et al. (2005)	118–307
					1–327
Pasture in mixed/tallgrass prairie, Little Washita, OK, USA	2 333	2 175	158	Meyers (2001); Gilmanov et al. (2003)	90–300
Northern mixed prairie, Fort Peck, MT, USA	459–1 455	996–1 293	− 537 to + 162	Gilmanov et al. (2005)	91–305
					138–302
Grassland steppe, no grazing, Shortandy, Kazakhstan	1 617	1 111	328–635	Gilmanov et al. (2004a)	124–306
Grassland steppe, grazed until 3 yr prior to study, southern Siberia			151	Marchesini et al. (2007)	117–274
Warm temperate grassland, Durham, NC, USA	4 407	4 763	− 356	Novick et al. (2004)	365
Tallgrass prairie, moderate seasonal grazing, Osage, OK, USA	2 787	3 039	− 252	Risser et al. (1981)	365
Spring wheat/barley, Shortandy, Kazakhstan	2 315	2 506	− 191	Current study	365
Wet artic tundra, Lena River Delta, northern Siberia			− 71	Kutzbach et al. (2007)	365
Tallgrass prairie, ungrazed, Osage, OK, USA	2 821	2 872	− 51	Risser et al. (1981)	365
Tallgrass prairie, moderate year-round grazing, Osage, OK, USA	3 678	3 698	− 19	Risser et al. (1981)	365
Crested-wheatgrass, cut and stored for hay, Shortandy, Kazakhstan	2 240	2 254	−14	Current study	365
Northern temperate grassland Lethbridge, Alberta, Canada	1 026	1 021	+5	Flanagan et al. (2002)	365
Seeded western wheatgrass, Mandan, ND, USA			− 131 to + 128	Frank (2002)	365
Grazed mixed-grass prairie, Mandan, ND, USA			− 70 to + 189	Frank (2002)	365
Grassland steppe, no grazing, Shortandy, Kazakhstan	2 521	23 68	153	Current study	365
Mediterranean grassland, Ione, CA, USA	2 926	2 737	189	Xu and Baldocchi (2004)	365
	2 673–3179	2 695–2 779	− 106–484		
Shortgrass prairie, control, CO, USA	1 945	1 545	400	Andrews et al. (1974); Coupland and Van Dyne (1979); Schultz (1995)	365
Mixed prairie, winter grazing, Woodward, OK, USA	3 037	2 517	520	Sims and Bradford (2001); Gilmanov et al. (2003)	365
Abandoned cropland, Shortandy, Kazakhstan	3 445	2 909	536	Current study	365
Tallgrass prairie, after spring burn, Shidler, OK, USA	5 223	3 964	1 259	Gilmanov et al. (2003)	365
Wide variety of grassland sites in 13 European countries	1 713–6 873	1 809–5 730	− 627–2 394	Gilmanov et al. (2007)	365

difference in area planted with wheat or barley in Kazakhstan between 1992 and 1999 (9 million ha, FAOSTAT 2008), a potential of 0.018 Pg of carbon could be released or captured annually, depending on whether these areas are cultivated or not. This amount of carbon represents 3.6% of the carbon potentially sequestered by grassland ecosystems globally (0.5 Pg carbon), as estimated by Scurlock and Hall (1998).

MANAGEMENT IMPLICATIONS

Combining micrometeorological and modeling techniques provided a quantitative assessment of CO_2 fluxes for major land-use types in northern Kazakhstan. WB exhibited high rates of CO_2 accumulation and high respiratory loss during a relatively short time period. AL had flux patterns similar to those of WB but had an overall higher carbon accumulation because of earlier growth initiation in the spring. VL and CW had relatively low GPP values, but NEE was positive throughout the growing season. This resulted in annual NEE values that were in the order AL > VL > CW > WB. SOC and nitrogen contents were highest for VL and decreased with greater degrees of cultivation.

Our results suggest that carbon and nitrogen lost by cultivation on VL are being partially restored when croplands are abandoned. Estimates of annual NEE for the four land-use types examined in our study allowed the calculation of the potential influence of land-use change on regional carbon balance. The difference in carbon captured by AL compared to cultivated cropland (WB) suggests that farmers could sell carbon credits when the fields are left uncultivated.

A more accurate estimation of the regional carbon balance would require estimates of the area covered by each land use and the integration of other factors that influence annual variations in soil carbon accumulation.

ACKNOWLEDGMENT

The authors thank the field assistants in Dr Akshalov's lab, who provided invaluable assistance during the field measurements.

LITERATURE CITED

Andrews, R., D. C. Coleman, J. E. Ellis, and J. S. Singh. 1974. Energy flow relationships in a shortgrass prairie ecosystem. Proceedings of the First

International Congress of Ecology. Wageningen, The Netherlands: Centre for Agricultural Publishing and Documentation. p. 22–28.

Chuluun, T., and D. Ojima. 2002. Land use change and carbon cycle in and semi-arid lands of east and central Asia. *Science in China Series C—Life Sciences* 45:48–54.

Coupland, R. T., and G. M. V. Dyne. 1979. Systems synthesis grassland ecosystems of the world. *In:* R. T. Coupland [ed.]. Grassland ecosystems of the world: analysis of grasslands and their uses. Oxford, United Kingdom: Oxford University Press. p. 97–106.

Emmerich, W. E. 2007. Ecosystem water use efficiency in a semiarid shrubland and grassland community. *Rangeland Ecology and Management* 60:464–470.

Falge, E., D. Baldocchi, R. Olson, P. Anthoni, M. Aubinet, C. Bernhofer, G. Burba, R. Ceulemans, R. Clement, H. Dolman, A. Granier, P. Gross, T. Grunwald, D. Hollinger, N. O. Jensen, G. Katul, P. Keronen, A. Kowalski, C. T. Lai, B. E. Law, T. Meyers, H. Moncrieff, E. Moors, J. W. Munger, K. Pilegaard, U. Rannik, C. Rebmann, A. Suyker, J. Tenhunen, K. Tu, S. Verma, T. Vesala, K. Wilson, and S. Wofsy. 2001. Gap filling strategies for defensible annual sums of net ecosystem exchange. *Agricultural and Forest Meteorology* 107:43–69.

FAOSTAT. 2008. FAO Statistical Databases. Available at: http://faostat.fao.org/. Accessed 9 April 2008.

Flanagan, L. B., L. A. Wever, and P. J. Carlson. 2002. Seasonal and interannual variation in carbon dioxide exchange and carbon balance in a northern temperate grassland. *Global Change Biology* 8:599–615.

Frank, A. B. 2002. Carbon dioxide fluxes over a grazed prairie and seeded pasture in the northern Great Plains. *Environmental Pollution* 116:397–403.

Gilmanov, T. G., D. A. Johnson, N. Z. Saliendra, K. Akshalov, and B. K. Wylie. 2004a. Gross primary productivity of the true steppe in Central Asia in relation to NDVI: scaling up CO_2 fluxes. *Environmental Management* 33:S492–S508.

Gilmanov, T. G., D. A. Johnson, N. Z. Saliendra, T. J. Svejcar, R. F. Angell, and K. L. Clawson. 2004b. Winter CO_2 fluxes above sagebrush-steppe ecosystems in Idaho and Oregon. *Agricultural and Forest Meteorology* 126:73–88.

Gilmanov, T. G., J. E. Soussana, L. Aires, V. Allard, C. Ammann, M. Balzarolo, Z. Barcza, C. Bernhofer, C. L. Campbell, A. Cernusca, A. Cescatti, J. Clifton-Brown, B. O. M. Dirks, S. Dore, W. Eugster, J. Fuhrer, C. Gimeno, T. Gruenwald, L. Haszpra, A. Hensen, A. Ibrom, A. F. G. Jacobs, M. B. Jones, G. Lanigan, T. Laurila, A. Lohila, G. Manca, B. Marcolla, Z. Nagy, K. Pilegaard, K. Pinter, C. Pio, A. Raschi, N. Rogiers, M. J. Sanz, P. Stefani, M. Sutton, Z. Tuba, R. Valentini, M. L. Williams, and G. Wohlfahrt. 2007. Partitioning European grassland net ecosystem CO_2 exchange into gross primary productivity and ecosystem respiration using light response function analysis. *Agriculture Ecosystems & Environment* 121:93–120.

Gilmanov, T. G., T. J. Svejcar, D. A. Johnson, R. F. Angell, N. Z. Saliendra, and B. K. Wylie. 2006. Long-term dynamics of production, respiration, and net CO_2 exchange in two sagebrush-steppe ecosystems. *Rangeland Ecology and Management* 59:585–599.

Gilmanov, T. G., L. L. Tieszen, B. K. Wylie, L. B. Flanagan, A. B. Frank, M. R. Haferkamp, T. P. Meyers, and J. A. Morgan. 2005. Integration of CO_2 flux and remotely-sensed data for primary production and ecosystem respiration analyses in the northern Great Plains: potential for quantitative spatial extrapolation. *Global Ecology and Biogeography* 14:271–292.

Gilmanov, T. G., S. B. Verma, P. L. Sims, T. P. Meyers, J. A. Bradford, G. G. Burba, and A. E. Suyker. 2003. Gross primary production and light response parameters of four Southern Plains ecosystems estimated using long-term CO_2-flux tower measurements. *Global Biogeochemical Cycles* 17(2):1071.

Harris, D., W. R. Horwath, and C. van Kessel. 2001. Acid fumigation of soils to remove carbonates prior to total organic carbon or carbon-13 isotopic analysis. *Soil Science Society of America Journal* 65:1853–1856.

Held, A. A., P. Steduto, F. Orgaz, A. Matista, and T. C. Hsiao. 1990. Bowen-ratio energy-balance technique for estimating crop net CO_2 assimilation, and comparison with a canopy chamber. *Theoretical and Applied Climatology* 42:203–213.

Hooper, D. U., Z. G. Cardon, F. S. Chapin, and M. Durant. 2002. Corrected calculations for soil and ecosystem measurements of CO_2 flux using the LI-COR 6200 portable photosynthesis system. *Oecologia* 132:1–11.

Irmak, S., D. Mutiibwa, A. Irmak, T. J. Arkebauer, A. Weiss, D. L. Martin, and D. E. Eisenhauer. 2008. On the scaling up leaf stomatal resistance to canopy resistance using photosynthetic photon flux density. *Agricultural and Forest Meteorology* 148:1034–1044.

Kutzbach, L., C. Wille, and E. M. Pfeiffer. 2007. The exchange of carbon dioxide between wet arctic tundra and the atmosphere at the Lena River Delta, Northern Siberia. *Biogeosciences* 4:869–890.

Laine, A., M. Sottocornola, G. Kiely, K. A. Byrne, D. Wilson, and E. S. Tuittila. 2006. Estimating net ecosystem exchange in a patterned ecosystem: example from blanket bog. *Agricultural and Forest Meteorology* 138:231–243.

LI-COR. 1987. The LI-6200 Primer. An introduction to operating the LI-6200 portable photosynthesis system. Lincoln, NE, USA: LI-COR Inc. 107 p.

LI-COR. 2001. Revisiting the LI-6200 equations. Application note 125. Lincoln, NE, USA: LI-COR Inc. 8 p.

Lloyd, J., and J. A. Taylor. 1994. On the temperature dependence of soil respiration. *Functional Ecology* 8:315–323.

Loomis, R. S., and D. J. Connor. 1992. Crop ecology: productivity and management in agricultural systems. Cambridge, United Kingdom: Cambridge University Press. 538 p.

Lotsch, A., Y. Tian, M. A. Friedl, and R. B. Myneni. 2003. Land cover mapping in support of LAI/FPAR retrievals from EOS MODIS and MISR. Classification methods and sensitivities to errors. *International Journal of Remote Sensing* 24:1997–2016.

Marchesini, L. B., D. Papale, M. Reichstein, N. Vuichard, N. Tchebakova, and R. Valentini. 2007. Carbon balance assessment of a natural steppe of southern Siberia by multiple constraint approach. *Biogeosciences* 4:581–595.

Mariko, S., N. Nishimura, W. H. Mo, Y. Matsui, T. Kibe, and H. Koizumi. 2000. Winter CO_2 flux from soil and snow surfaces in a cool-temperate deciduous forest, Japan. *Ecological Research* 15:363–372.

Meyers, T. P. 2001. A comparison of summertime water and CO_2 fluxes over rangeland for well watered and drought conditions. *Agricultural and Forest Meteorology* 106:205–214.

Novick, K. A., P. C. Stoy, G. G. Katul, D. S. Ellsworth, M. B. S. Siqueira, J. Juang, and R. Oren. 2004. Carbon dioxide and water vapor exchange in a warm temperate grassland. *Oecologia* 138:259–274.

Ohkubo, S., Y. Kosugi, S. Takanashi, T. Mitani, and M. Tani. 2007. Comparison of the eddy covariance and automated closed chamber methods for evaluating nocturnal CO_2 exchange in a Japanese cypress forest. *Agricultural and Forest Meteorology* 142:50–65.

Olson, D. M., E. Dinerstein, E. D. Wikramanayake, N. D. Burgess, G. V. N. Powell, E. C. Underwood, J. A. D'Amico, I. Itoua, H. E. Strand, J. C. Morrison, C. J. Loucks, T. F. Allnutt, T. H. Ricketts, Y. Kura, J. F. Lamoreux, W. W. Wettengel, P. Hedao, and K. R. Kassem. 2001. Terrestrial ecoregions of the world: a new map of life on Earth. *Bioscience* 51:933–938.

Reichstein, M., E. Falge, D. Baldocchi, D. Papale, M. Aubinet, P. Berbigier, C. Bernhofer, N. Buchmann, T. Gilmanov, A. Granier, T. Grunwald, K. Havrankova, H. Ilvesniemi, D. Janous, A. Knohl, T. Laurila, A. Lohila, D. Loustau, G. Matteucci, T. Meyers, F. Miglietta, J. M. Ourcival, J. Pumpanen, S. Rambal, E. Rotenberg, M. Sanz, J. Tenhunen, G. Seufert, F. Vaccari, T. Vesala, D. Yakir, and R. Valentini. 2005. On the separation of net ecosystem exchange into assimilation and ecosystem respiration: review and improved algorithm. *Global Change Biology* 11:1424–1439.

Risch, A. C., and D. A. Frank. 2006. Carbon dioxide fluxes in a spatially and temporally heterogeneous temperate grassland. *Oecologia* 147:291–302.

Risser, P. G., E. C. Birney, H. D. Blocker, S. W. May, W. J. Parton, and J. A. Wiens. 1981. The true prairie ecosystem. Stroudsburg, PA, USA: Hutchinson Ross. 557 p.

SAS. 2001. SAS/STAT 9.1 user's guide. Cary, NC, USA: SAS Institute Inc. p. 2997–3044.

Schimel, D. S., J. I. House, K. A. Hibbard, P. Bousquet, P. Ciais, P. Peylin, B. H. Braswell, M. J. Apps, D. Baker, A. Bondeau, J. Canadell, G. Churkina, W. Cramer, A. S. Denning, C. B. Field, P. Friedlingstein, C. Goodale, M. Heimann, R. A. Houghton, J. M. Melillo, B. Moore, D. Murdiyarso, I. Noble, S. W. Pacala, I. C. Prentice, M. R. Raupach, P. J. Rayner, R. J. Scholes, W. L. Steffen, and C. Wirth. 2001. Recent patterns and mechanisms of carbon exchange by terrestrial ecosystems. *Nature* 414:169–172.

Schultz, J. 1995. The ecozones of the world: the ecological divisions of the geosphere. Berlin, Germany: Springer-Verlag. 456 p.

Schuman, G. E., H. H. Janzen, and J. E. Herrick. 2002. Soil carbon dynamics and potential carbon sequestration by rangelands. *Environmental Pollution* 116:391–396.

Scurlock, J. M. O., and D. O. Hall. 1998. The global carbon sink: a grassland perspective. *Global Change Biology* 4:229–233.

Sims, P. L., and J. A. Bradford. 2001. Carbon dioxide fluxes in a southern plains prairie. *Agricultural and Forest Meteorology* 109:117–134.

Smith, E. L. 1938. Limiting factors in photosynthesis: light and carbon dioxide. *The Journal of General Physiology* 22:21–35.

Tropicos.org. 2008. Missouri Botanical Garden, St. Louis, MO, USA. Available at: http://www.tropicos.org. Accessed 8 November 2009.

World Resources Institute. 2000. World resources 2000–2001: people and ecosystems: the fraying web of life. Washington, DC, USA: World Resources Institute, United Nations Development Programme, The United Nations Environment Programme, and the World Bank. 389 p.

Xu, L. K., and D. D. Baldocchi. 2004. Seasonal variation in carbon dioxide exchange over a Mediterranean annual grassland in California. *Agricultural and Forest Meteorology* 123:79–96.

Zhang, W. L., S. P. Chen, J. Chen, L. Wei, X. G. Han, and G. H. Lin. 2007. Biophysical regulations of carbon fluxes of a steppe and a cultivated cropland in semiarid Inner Mongolia. *Agricultural and Forest Meteorology* 146:216–229.

Zhao, F. H., G. R. Yu, S. G. Li, C. Y. Ren, X. M. Sun, N. Mi, J. Li, and Z. Ouyang. 2007. Canopy water use efficiency of winter wheat in the North China Plain. *Agricultural Water Management* 93:99–108.